pH-Dependent Charge Equilibria between Tyrosine-D and the S States in Photosystem II. Estimation of Relative Midpoint Redox Potentials†

Imre Vass*,‡ and Stenbjörn Styring
Department of Biochemistry, Arrhenius Laboratories for Natural Sciences, Stockholm University, 106 91 Stockholm, Sweden
Received May 17, 1990; Revised Manuscript Received August 31, 1990

ABSTRACT: The effect of protonation events on the charge equilibrium between tyrosine-D and the water-oxidizing complex in photosystem II has been studied by time-resolved measurements of the EPR signal II_{slow} at room temperature. The flash-induced oxidation of Y_D by the water-oxidizing complex in the S_2 state is a monophasic process above pH 6.5 and biphasic at lower pHs, showing a slow and a fast phase. The half-time of the slow phase increases from about 1 s at pH 8.0 to about 20 s at pH 5.0, whereas the half-time of the fast phase is pH independent (0.4–1 s). The dark reduction of Y_D^+ was followed by measuring the decay of signal II_{slow} at room temperature. Y_D^+ decays in a biphasic way on the tens of minutes to hours time scale. The minutes phase is due to the electron transfer to Y_D^+ from the S_0 state of the water-oxidizing complex. The half-time of this process increases from about 5 min at pH 8.0 to 40 min at pH 4.5. The hours phase of Y_D^+ has a constant half-time of about 500 min between pH 4.7 and 7.2, which abruptly decreases above pH 7.2 and below pH 4.7. This phase reflects the reduction of Y_D^+ either from the medium or by an unidentified redox component of PSII in those centers that are in the S_1 state. The titration curve of the half-times for the oxidation of Y_D reveals a proton binding with a pK around 7.3–7.5 that retards the electron transfer from Y_D to the water-oxidizing complex. We propose that this monoprotic event reflects the protonation of an amino acid residue, probably histidine-190 on the D2 protein, to which Y_D is hydrogen bonded. The titration curves for the oxidation of Y_D and for the reduction of Y_D^+ show a second proton binding with p$K \approx 5.8$–6.0 that accelerates the electron transfer from Y_D to the water-oxidizing complex and retards the process in the opposite direction. This protonation most probably affects the water-oxidizing complex. From the measured kinetic parameters, the lowest limits for the equilibrium constants between the $S_0Y_D^+$ and the S_1Y_D as well as between the $S_1Y_D^+$ and S_2Y_D states were estimated to be 5 and 750–1000, respectively. These equilibrium constants permitted us to derive a relative redox potential scheme showing that the S_1/S_0 redox couple of the water-oxidizing complex is at least 40 mV more negative than the Y_D^+/Y_D couple and the latter is at least 170 mV more negative than the S_2/S_1 redox couple of the water-oxidizing complex. Together with available data in the literature, these estimations place the Y_D^+/Y_D couple at approximately 720–760 mV.

Photosystem II (PSII)[1] is a multifunctional pigment–protein complex in the thylakoid membrane that catalyzes the light-induced oxidation of water and the reduction of plastoquinone [for recent reviews see Babcock (1987), Andreasson & Vänngård (1988), Brudvig et al. (1989), and Hansson & Wydrzynski (1990)]. The reaction center of PSII is constituted by a heterodimer of the hydrophobic proteins D1 and D2 that binds the primary electron donor P_{680}, the intermediary electron acceptor pheophytin, and the primary (Q_A) and secondary (Q_B) quinone acceptors (Nanba & Satoh, 1987). Recent evidence suggests that the catalytic Mn cluster of the water-oxidizing complex is also bound to the D1/D2 heterodimer (Andersson et al., 1987; Virgin et al., 1988; Seibert et al., 1989; Mei et al., 1989; Svensson et al., 1990). During illumination, the water-oxidizing complex cycles through five redox states denoted S_0, ..., S_4, releasing molecular oxygen in the S_3–S_4–S_0 transition (Kok et al., 1970). S_0 represents the most reduced state, while the higher S states represent successively higher oxidation states. The oxidative power in the higher S states is stored, at least partially, on Mn ions constituting the catalytic site of water oxidation.

In addition to the bound redox components, both the D1 and the D2 proteins contain a redox-active tyrosine residue, denoted as Y_Z and Y_D, respectively. Y_Z is tyrosine-161 on the D1 protein (Debus et al., 1988b; Metz et al., 1989), and Y_D is tyrosine-160 in the D2 protein (Debus et al., 1988a; Vermaas et al., 1988). Oxidation of the tyrosines give rise to characteristic EPR spectra called signal $II_{very\ fast}$ from Y_Z^+ (Blankenship et al., 1975) and signal II_{slow} from Y_D^+ (Babcock & Sauer, 1973). The EPR signals decay with different kinetics (hence the denotations "very fast" and "slow") but have in other respects very similar spectral characteristics indicative of a similar protein environment around the two tyrosines (Babcock et al., 1989; Svensson et al., 1990). The spectra have recently been assigned to the neutral, deprotonated form of the tyrosine radicals (Babcock et al., 1989). The functions of Y_Z and Y_D are quite different. Y_Z is the intermediate electron carrier between P_{680} and the Mn cluster. After a flash,

† I.V. was supported by the Swedish Natural Science Research Council. S.S. was the recipient of a long-term grant for biotechnological basic research financed by the Knut and Alice Wallenbergs Foundation, Stockholm, Sweden. The work was supported by the Swedish Natural Science Research Council, the Knut and Alice Wallenbergs Foundation, and the Erna and Victor Hasselblad Foundation.

‡ On leave from the Institute of Plant Physiology, Biological Research Center of the Hungarian Academy of Sciences, Szeged, Hungary.

[1] Abbreviations: DCPIP, 2,6-dichlorophenolindophenol; Hepes, 4-(2-hydroxyethyl)-1-piperazineethanesulfonic acid; Mes, 4-morpholineethanesulfonic acid; P_{680}, primary electron donor of PSII; PSII, photosystem II; Q_A, primary quinone acceptor of PSII; Q_B, secondary quinone acceptor of PSII; Y_Z, tyrosine-161 on the D1 protein, electron carrier between P_{680} and the water-oxidizing complex; Y_D, tyrosine-160 on the D2 protein, accessory electron donor in PSII; PPBQ, phenyl-*p*-benzoquinone; S_0–S_4, charge storage states of the water-oxidizing complex.

0006-2960/91/0430-830$02.50/0

Scheme I: Charge Equilibria between Y_D/Y_D^+ and the Different S States[a]

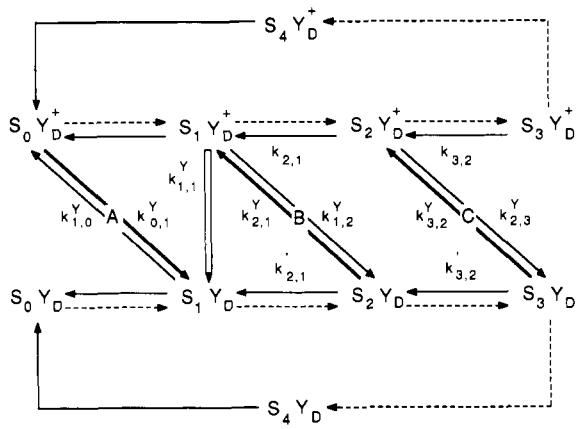

[a] Dashed arrows indicate the light-induced S-state transitions, and solid arrows represent the electron transfer steps that occur in the dark with k_{ij} rate constants. Here the indices i and j correspond to the S states where the reaction starts and ends, respectively. The superscript Y indicates that a redox change of Y_D is involved in the process. The bold arrows (A–C) symbolize the displacement of the equilibria. In the present study, reactions A and B and the reduction of Y_D^+ in the $S_1Y_D^+$ centers have been measured. In the latter case, the $S_1Y_D^+$ centers may be converted to S_1Y_D centers either directly (open arrow) or via the S_2Y_D state as discussed in the text.

it is oxidized by P_{680}^+ in the 20–200-ns time scale (Brettel et al., 1984) and reduced by electrons extracted from the water-oxidizing complex in the microseconds to milliseconds time scale (Rutherford, 1989). During illumination, Y_D also becomes oxidized. Contrary to Y_Z^+, however, Y_D^+ is stable in the dark for minutes to hours (Lozier & Butler, 1973; Babcock & Sauer, 1973). Although Y_D is not involved in the steady-state electron transfer that leads to water oxidiation, it is in a complex charge equilibrium with the water-oxidizing complex. These reactions are summarized in Scheme I. In the light, Y_D is oxidized in all centers (Scheme I, upper half) and the $S_0Y_D^+$, ..., $S_3Y_D^+$ states are evenly populated. After the light is switched off, $S_3Y_D^+$ and $S_2Y_D^+$ decay back to $S_1Y_D^+$ ($k_{3,2}$ and $k_{2,1}$), resulting in approximately 25% $S_0Y_D^+$ and 75% $S_1Y_D^+$ after 3–5 min of dark adaptation. During further dark adaptation, the $S_0Y_D^+$ centers are converted to S_1Y_D centers ($k^Y_{0,1}$) in tens of minutes (Vermaas et al., 1984; Styring & Rutherford, 1987; Vass et al., 1990a). This equilibrium reaction is represented by A in Scheme I, and it is largely displaced in the direction of the bold arrow. When the samples are kept in darkness for hours, Y_D^+ is reduced in the S_1 centers as well (Babcock & Sauer, 1973), converting the majority of the centers to the S_1Y_D state as shown by the unfilled arrow in Scheme I ($k^Y_{1,1}$). Illumination of dark-adapted samples induces S-state turnovers in all centers. The formation of S_2Y_D and S_3Y_D is followed by their conversion to $S_1Y_D^+$ and $S_2Y_D^+$, respectively (Babcock & Sauer, 1973; Velthuys & Visser, 1975; Vermaas et al., 1984; Styring & Rutherford, 1987; Vass et al., 1990a), in the seconds time scale ($k^Y_{2,1}$, $k^Y_{3,2}$). These reactions (equilibria B and C in Scheme I, which are displaced in the direction of the bold arrows) eventually result in the complete oxidation of Y_D.

The midpoint redox potentials of the tyrosine radicals and the S states are of great importance. $E_m(Y_D^+/Y_D)$ was suggested to be at around 760 mV (Boussac & Etienne, 1984) or 490 mV (Tso et al., 1987) from redox titrations using strong oxidants, which, however, might have changed the protein surroundings, influencing the redox characteristics of Y_D. The oxidation of Y_D by the S_2 and S_3 states and the reduction of Y_D^+ by the S_0 state (Scheme I) indicates that $E_m(Y_D^+/Y_D)$ is more positive than $E_m(S_1/S_0)$ and more negative than $E_m(S_2/S_1)$ and $E_m(S_3/S_2)$ (Styring & Rutherford, 1987). However, the exact redox potential differences are not known.

Protolytic events are strongly coupled with many of the electron transport steps in PSII, which therefore have pH-dependent rate constants. The successive redox transitions $S_0 \rightarrow S_1 \rightarrow S_2 \rightarrow S_3 \rightarrow S_0$ are accompanied by the release of one, zero, one, and two protons, respectively, when measured around pH 7.0 (Fowler, 1977). Protolytic reactions are also involved at the level of Y_Z. Upon oxidation of Y_Z, a transient proton release was observed that was interpreted as indicating a pK shift of a proteinaceous group in the vicinity of Y_Z (Renger & Völker, 1982; Förster & Junge, 1984). It was also shown that the rate of the electron transfer between Y_Z and P_{680}^+ is retarded by lowering the bulk pH both in purified PSII reaction centers with intact water-oxidizing complex (Meyer et al., 1989) and in Tris-washed PSII membranes (Conjeaud & Mathis, 1986) where the water-oxidizing complex is removed.

The chemical nature and the protein environment of Y_Z and Y_D are very similar, which suggests that protolytic processes may play an important role in the redox reactions of Y_D as well. Here we have investigated the pH dependence of the electron transfer kinetics between Y_D and the water-oxidizing complex. We have observed the binding of two protons with pK 5.8–6.0 and 7.3–7.5 that inversely influence the rate of the electron transfer between Y_D and the Mn cluster. We have also estimated the relative midpoint redox potential differences between Y_D and the different S states.

Materials and Methods

Sample Preparation. PSII-enriched membranes (BBY particles) were prepared from spinach thylakoids (Berthold et al., 1981; Franzen et al., 1985) and were stored at −80 °C until use in a buffer of 0.4 M sucrose, 15 mM NaCl, 5 mM $MgCl_2$, and 20 mM Mes, pH 6.3, at 3–4 mg of Chl/mL. Y_D^+ was reduced by the addition of 3 mM sodium ascorbate and 0.3 mM DCPIP to BBY particles at 1 mg of Chl/mL. After 10 min of dark incubation on ice, the chemicals were removed by repeated dilution and centrifugation. For the EPR measurements, the BBY particles were spun down and then resuspended in either 50 mM L-glutamic acid (pH 4.5–5.0), Mes (pH 5.0–7.0), Hepes (pH 7.0–8.0), or glycylglycine (pH = 8.0–8.5) buffers with the same additions as indicated above. All sample manipulations were performed in darkness.

EPR Measurements. Room temperature (21 °C) EPR measurements were done in a 330-μL quartz flat cell at 1.5–2.0 mg of Chl/mL. The light-induced oxidation of Y_D was induced by one 300-ns flash from a Candela dye laser (λ = 590 nm; Rhodamin-6G) directed into the EPR cavity. The formation of Y_D^+ (in the seconds time scale) was followed by measuring the rise kinetics of signal II_{slow} at its low-field peak with a Bruker ESP 300 spectrometer equipped with a Bruker 8102 standard cavity. Data acquisition was performed with the ESP 300 program of the EPR spectrometer. Exponential analysis of the kinetic traces was done with an IBM AT computer using a least-squares curve-fitting program. The very slow dark decay of Y_D^+ (in the hours time scale) was monitored by measuring the full spectrum of signal II_{slow} every 3–6 min by using an automation routine of the ESP 300 program. From those spectra the intensity of signal II_{slow} was obtained. No sedimentation of the samples occurred during the measurements.

Oxygen Evolution Measurements. The oxygen-evolving activity of the samples was measured in the same buffers as those used for the EPR measurements with a Hansatech

Scheme II

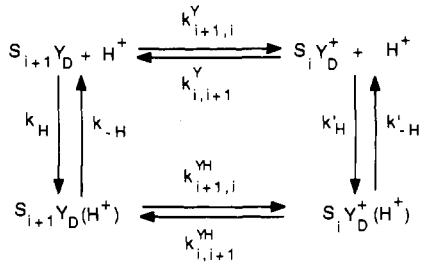

Clark-type oxygen electrode at 10 μg of Chl/mL in the presence of 1 mM PPBQ. Before the measurements, the samples were incubated for 2 min in the dark in the appropriate buffer.

Analysis of Y_D/Y_D^+ Oxidation/Reduction Kinetics. In Scheme I, we did not take into account the effect of protonation on the electron transfer between Y_D (Y_D^+) and the water-oxidizing complex. However, this is necessary to correctly describe the electron transfer kinetics. Scheme II summarizes the coupling of redox and protolytic equilibria between Y_D and the S states. Scheme II in general results in complicated multiphasic kinetics for the oxidation/reduction of Y_D/Y_D^+ with pH-dependent rate constants and amplitudes. However, the complicated picture can be simplified by taking into account the special characteristics of the studied system.

(1) Oxidation of Y_D by the S_2 State. In this case, the redox equilibria shown in Scheme II are displaced very much to the right (see later). Thus, the reversed reaction, i.e., the reduction of Y_D^+ by the S_1 state, has negligible effect on the kinetics of Y_D^+ formation. From this condition it also follows that the proton equilibrium between the $S_iY_D^+$ and $S_iY_D^+(H^+)$ centers does not influence the rate of Y_D^+ formation. With respect to the effect of proton equilibrium between the $S_{i+1}Y_D$ and the $S_{i+1}Y_D(H^+)$ centers, we will discuss two important limiting cases:

(A) Slow Proton Equilibrium. In this case, the rate of proton binding and release is much slower than the rate of electron transfer. Thus, there is no exchange between the protonated and unprotonated centers on the time scale of the measurements. The kinetic equations of Y_D oxidation on the basis of Scheme II in the case of slow proton equilibrium are

$$\frac{d[S_{i+1}Y_D]}{dt} = -k^{Y}_{i+1,i}[S_{i+1}Y_D] \quad (1a)$$

$$\frac{d[S_{i+1}Y_D(H^+)]}{dt} = -k^{YH}_{i+1,i}[S_{i+1}Y_D(H^+)] \quad (1b)$$

$$\frac{d[Y_D^+]}{dt} = k^{Y}_{i+1,i}[S_{i+1}Y_D] + k^{YH}_{i+1,i}[S_{i+1}Y_D(H^+)] \quad (1c)$$

where $[Y_D^+] = [S_iY_D^+] + [S_iY_D^+(H^+)]$ is the total concentration of oxidized tyrosine-D detected by the EPR measurement of signal II_{slow}. The solution of the set of eqs 1a–c results in biphasic kinetics, with pH-independent time constants, for the increase of Y_D^+ concentration as a function of time:

$$[Y_D^+(t)] - [Y_D^+(0)] = A(1 - e^{-k^{Y}_{i+1,i}t}) + B(1 - e^{-k^{YH}_{i+1,i}t}) \quad (2a)$$

In this expression, the amplitudes are pH dependent:

$$A = [Y_D(0)]/(1 + 10^{pK-pH}) \quad (2b)$$

$$B = [Y_D(0)]10^{pK-pH}/(1 + 10^{pK-pH}) \quad (2c)$$

where $[Y_D(0)] = [S_{i+1}Y_D(0)] + [S_{i+1}Y_D(H^+)(0)]$ is the concentration of reduced tyrosine-D at the moment of the flash illumination and pK refers to the proton equilibrium between the $S_{i+1}Y_D$ and $S_{i+1}Y_D(H^+)$ centers.

(B) Fast Proton Equilibrium. In this case, the rate of proton binding and release is much faster than the rate of electron transfer. Thus, there is always a fast exchange and, in turn, an equilibrium between the unprotonated and protonated forms of the reduced complex, i.e., $k_H[H^+][S_{i+1}Y_D] = k_{-H}[S_{i+1}Y_D(H^+)]$. The kinetic equations for the oxidation of Y_D in the case of fast proton equilibrium are

$$\frac{d[Y_D]}{dt} = -k'[Y_D] \quad (3a)$$

$$\frac{d[Y_D^+]}{dt} = k'[Y_D] \quad (3b)$$

where k' is a pH-dependent rate constant:

$$k' = (k^{YH}_{i+1,i} + k^{Y}_{i+1,i}10^{pH-pK})/(1 + 10^{pH-pK}) \quad (4)$$

The increase in the amount of the oxidized tyrosine-D as a function of time is described by monophasic kinetics with pH-dependent rate constant k':

$$[Y_D^+(t)] - [Y_D^+(0)] = [Y_D(0)]\,(1 - e^{-k't}) \quad (5)$$

(2) Reduction of Y_D^+ by the S_0 State. In this case, the redox equilibrium shown in Scheme II is displaced to the left (see later). Thus, the oxidation of Y_D by the S_1 state is negligible, and consequently the proton equilibrium between the $S_{i+1}Y_D$ and $S_{i+1}Y_D(H^+)$ centers does not affect the rate of the reduction of Y_D^+. With respect to the proton equilibrium between the $S_iY_D^+$ and $S_iY_D^+(H^+)$ centers, we will discuss two limiting cases:

(A) Slow Proton Equilibrium. In this case, the rate of proton binding and release is slow compared to the rate of the electron transfer; thus, there is no coupling between the decay of Y_D^+ in the protonated and nonprotonated centers. The kinetic equations for the reduction of Y_D^+ in the case of slow proton equilibrium are

$$\frac{d[S_iY_D^+]}{dt} = -k^{Y}_{i,i+1}[S_iY_D^+] \quad (6a)$$

$$\frac{d[S_iY_D^+(H^+)]}{dt} = -k^{YH}_{i,i+1}[S_iY_D^+(H^+)] \quad (6b)$$

The solution of the set of eqs 6a,b results in biphasic decay of Y_D^+ with pH-independent rate constants and pH-dependent amplitudes:

$$[Y_D^+(t)] = Ae^{-k^{Y}_{i,i+1}t} + Be^{-k^{YH}_{i,i+1}t} \quad (7a)$$

$$A = [Y_D^+(0)]/(1 + 10^{pK'-pH}) \quad (7b)$$

$$B = [Y_D^+(0)]10^{pK'-pH}/(1 + 10^{pK'-pH}) \quad (7c)$$

where $[Y_D^+(0)]$ is the total concentration of oxidized tyrosine-D at the beginning of its dark decay. pK' refers to the proton equilibrium between the $S_iY_D^+$ and $S_iY_D^+(H^+)$ centers.

(B) Fast Proton Equilibrium. In this case, the rate of proton equilibrium is fast compared to the rate of electron transfer. Thus, the protonated and unprotonated centers are in equilibrium throughout the reaction, i.e., $k'_H[H^+][S_iY_D^+] = k'_{-H}[S_iY_D^+(H^+)]$. The reduction kinetics of Y_D^+ in the case of fast proton equilibrium are described by

$$\frac{d[Y_D^+]}{dt} = -k''[Y_D^+] \quad (8)$$

where k'' is a pH-dependent rate constant:

$$k'' = (k^{YH}_{i,i+1} + k^{Y}_{i,i+1}10^{pH-pK'})/(1 + 10^{pH-pK'}) \quad (9)$$

The solution of eq 8 gives a monophasic decay for Y_D^+ with

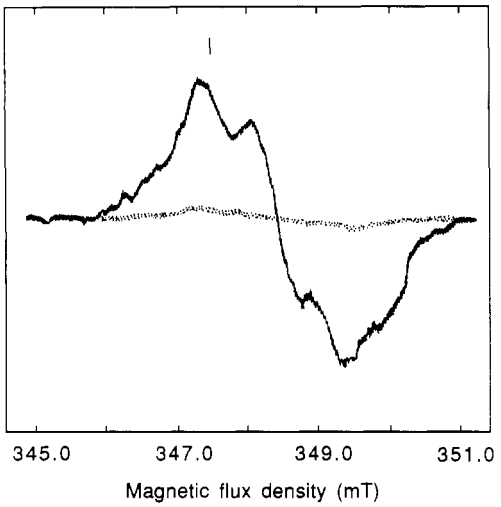

FIGURE 1: EPR spectra of signal II_{slow} in isolated BBY particles. BBY particles were washed with 0.3 mM DCPIP in the presence of 3.0 mM ascorbate to reduce Y_D^+. Signal II_{slow} was measured in the dark (dotted spectrum) and after illumination with a saturating laser flash (solid spectrum). The bar indicates the field position used in the kinetic measurements. EPR conditions: T = 294 K; microwave power, 10 dB below 200 mW; modulation amplitude, 0.5 mT; microwave frequency, 9.779 GHz.

pH-independent amplitude and pH-dependent rate constant k'':

$$[Y_D^+(t)] = [Y_D^+(0)]e^{-k''t} \quad (10)$$

Results and Discussion

Oxidation of Y_D by the S_2 State. Treatment of BBY particles with DCPIP/ascorbate reduces Y_D^+ as shown by the loss of signal II_{slow} (Figure 1, dotted spectrum). Illumination of these samples with a single saturating flash at room temperature is sufficient to oxidize the majority of Y_D as shown by the restoration of signal II_{slow} (Figure 1, solid spectrum). This is due to the reaction $S_2Y_D \rightarrow S_1Y_D^+$ (Scheme I, reaction B).

The room-temperature kinetics for the oxidation of Y_D after one flash were measured by monitoring the increase of signal II_{slow} at its low-field peak (indicated with a bar in Figure 1). Figure 2 shows the flash-induced signal II_{slow} formation between pH 7.5 and 4.7. The solid lines represent the best-fit theoretical curves obtained by using eq 5 or 2a for monophasic (Figure 2a) or biphasic (Figure 2b–d) kinetics, respectively. The oxidation kinetics are strongly pH dependent. At pH 7.5, the rise of signal II_{slow} is monophasic with about a 1-s half-time (Figure 2a), in agreement with earlier results obtained in thylakoids (Babcock & Sauer, 1973; Velthuys & Visser, 1975). At lower pHs, the kinetics are biphasic with a fast ($t_{1/2}$ = 0.4–1 s) and a slow phase ($t_{1/2}$ = 5–20 s) as shown in Figure 2b–d. Biphasic oxidation kinetics of Y_D have been reported earlier at pH 6.3 in BBY particles (Styring & Rutherford, 1987). However, they observed a longer half-time of the slow phase (30–40 s at pH 6.3 compared to 6–8 s in our study), which probably was caused by the lower "room temperature" during their measurements. At lower pHs, the amount of single-flash induced signal II_{slow} was significantly reduced (Figure 2) although the *total* amount of signal II_{slow} that could be induced by continuous illumination was constant between pH 4.5 and 8.5 (not shown).

Figure 3 summarizes the pH dependence of the kinetics of the single-flash induced oxidation of Y_D by the S_2 state. The half-time of the slow phase is about 1 s at pH 8.0 and increases to 15–20 s at pH 5.0 (Figure 3A). This effect can be explained by the binding of a proton, in fast equilibrium

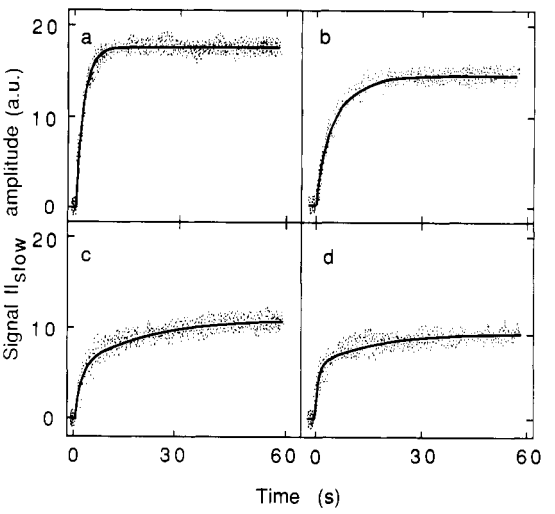

FIGURE 2: Signal II_{slow} formation after one flash at different pHs in BBY particles. BBY particles were treated with DCPIP/ascorbate to reduce Y_D^+ as indicated under Figure 1. The samples were illuminated with a single saturating laser flash in the cavity of the EPR spectrometer. The oxidation of Y_D was followed by measuring the rise kinetics of signal II_{slow} at its low-field peak (see Figure 1) at different pHs: a, pH 7.5; b, pH 6.3; c, pH 5.2; and d, pH 4.7. EPR conditions: T = 294 K; field, 347.4 mT; microwave power, 10 dB below 200 mW; modulation amplitude, 0.5 mT; microwave frequency, 9.779 GHz; conversion time, 40 ms; time constant, 40 ms; resolution, 80 ms/point.

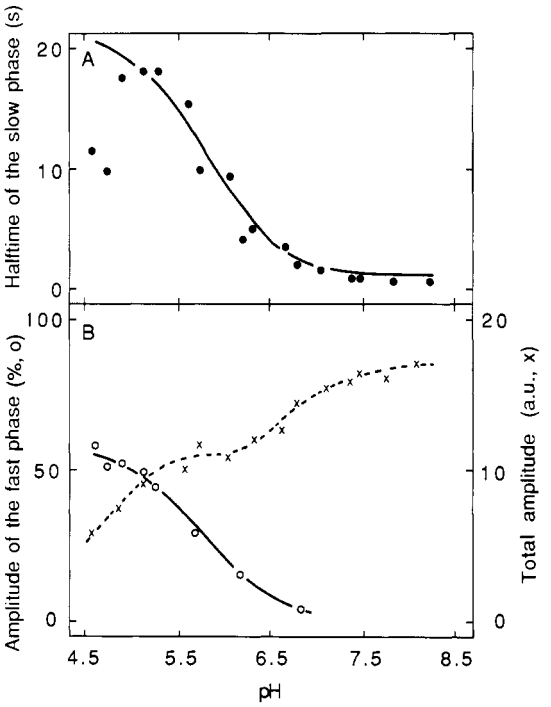

FIGURE 3: pH dependence of the kinetics of signal II_{slow} formation after one-flash illumination in BBY particles. BBY particles were treated with DCPIP/ascorbate and the formation of signal II_{slow} was measured at various pHs as shown in Figure 2. (A) The half-time of the slow phase of signal II_{slow} formation as a function of pH. The solid curve represents the best fit for a one-proton titration curve with pK 7.3. (B) (×) Total amplitude of signal II_{slow} induced by the flash. (○) Relative amplitude of the fast phase.

with the bulk solution, that retards the electron transfer from Y_D to the water-oxidizing complex. Fitting of the experimental data by using eq 4 results in pK 7.3 for the proton binding. The calculated curve describes well the measured half-times between pH 8.5 and 5.0 (Figure 3A, solid line) but deviates from the measured data below pH 5.0. The reason for this deviation is not known. However, it might be correlated with

the low-pH induced change of the water-oxidizing complex that inhibits oxygen evolution (see later and also in Figure 4). The rise kinetics of signal II_{slow} are biphasic below pH 7.0, and a fast phase with an essentially pH-independent half-time of 0.4–1 s grows in by lowering the pH. Its amplitude reaches a maximum of about 60% of the total amplitude of signal II_{slow} induced by the flash at pH 4.5 (Figure 3B, ○). The kinetics of this fast phase suggest the occurrence of a second proton binding that accelerates the electron transfer from Y_D to the water-oxidizing complex. The pH-dependent amplitude and the almost constant half-time of this phase show that the involved proton is in a slow equilibrium with the bulk solution on the seconds time scale of the measurements. The pH dependence of the amplitude of the fast phase was fitted by using eq 2c. The calculated titration curve (solid line in Figure 3B) results in pK 5.8 for the proton binding.

What is then the nature of the two protons that inversely affect the electron transfer from Y_D to the S_2 state? One plausible explanation for the retardation of the electron transfer from Y_D to the the water-oxidizing complex is an electrostatic effect induced by the binding of a proton with pK 7.3 in the vicinity of Y_D. The titrable group is unlikely to be on Y_D itself because its pK values are expected to be at around 10 and −1 for the reduced and oxidized forms, respectively (Babcock et al., 1989). Recent experiments have provided evidence for the involvement of the phenol oxygen of Y_D in a hydrogen bridge with a neighboring amino acid residue (Rodriguez et al., 1987; Evelo et al., 1989a). These experiments, however, also showed that the proton in the hydrogen bond is very firmly bound and extremely resistant to exchange with the bulk protons (Rodriguez et al., 1987). Thus, the hydrogen-bonded phenolic proton cannot be responsible for the fast protonation observed in our experiments. However, an indication to the nature of the proton-binding group came from recent computer modeling studies on the structure of the donor-side components of PSII. These studies showed that a highly likely candidate for the residue that forms a hydrogen bond with Y_D is His-190 of the D2 protein (Svensson et al., 1990). The measured pK of 7.3 is in the range where histidine residues often titrate, and we suggest that the protonation of His-190 of the D2 protein affects the rate of electron transfer from Y_D to the water-oxidizing complex. When the histidine is deprotonated (pH > 7.3) the reaction is fast, but after protonation of the histidine (pH < 7.3) the extra positive charge located close to Y_D slows down the electron transfer.

The appearance of the fast phase in the oxidation of Y_D indicates that an independent protonation event occurs with pK 5.8 that accelerates electron transfer from Y_D to the water-oxidizing complex. We suggest that the involved protonizable group is located at or near the water-oxidizing complex. When the group is protonated (pH < 5.8), the electron transfer from Y_D to the S_2 state is fast, and the fast phase dominates. When the group is deprotonated (pH > 5.8), the amplitude of the fast phase is decreased, and the slow phase will dominate. We cannot address the nature of the titrable group, but there is precedence for its existence in the literature. Meyer et al. (1989) suggested that a single proton binding with pK 5.3 at or near the water-oxidizing complex retards electron transfer from Y_Z to P_{680}^+ due to electrostatic interaction. Although the pK value obtained by us is somewhat higher (pK 5.8 compared to pK 5.3), we suggest that the same protonation event also accelerates the electron transfer from Y_D to the S_2 state. Our results agree with the findings of Meyer et al. (1989) also in that this protonation affects only about 60% of the centers. The cause of the inhomogeneous proton binding

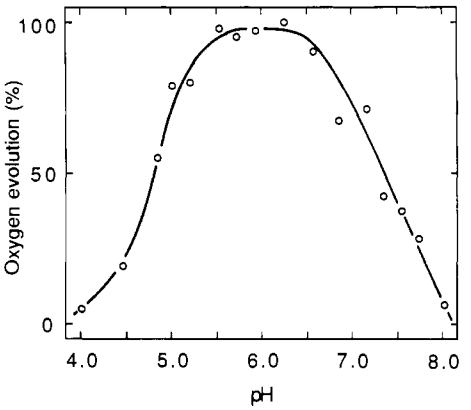

FIGURE 4: pH dependence of the steady-state oxygen evolution in BBY particles. The oxygen evolution was measured at various pHs with 1 mM PPBQ as electron acceptor.

is not known at present. However, it might be correlated with the two different forms of the water-oxidizing complex in the S_2 state: one giving rise to the S_2-state multiline EPR signal (Dismukes & Siderer, 1980) and the other to the S_2-state g = 4.1 EPR signal (Casey & Sauer, 1984; Zimmermann & Rutherford, 1984; Hansson et al., 1987).

The total amplitude of signal II_{slow} induced by a single flash declines upon lowering the pH (Figure 3B, ×). This is due to two different reactions. In our BBY particles, the size of the plastoquinone pool is limited; therefore, the flash results in the formation of Q_A^- in about 30–40% of the centers. In these centers Q_A^- and Y_D compete to donate an electron to the S_2 state. The half-time of the $S_2Q_A^-$ recombination is pH dependent. It increases from about 1–2 s observed between pH 6.0 and 7.0 to 5 s at pH 8.0 (Robinson & Crofts, 1984) and reaches about 20 s at pH 8.8 (Vass & Inoue, 1986). Our results show that the half-time of the electron donation from Y_D to the S_2 state changes with pH in the opposite way. It is about 1 s at pH 8.0 and increases to 10 s at pH 6.0. Thus, at high pH Y_D is a much more efficient donor to the S_2 state than Q_A^-, and the $S_2Y_D \rightarrow S_1Y_D^+$ reaction will dominate after the flash. However, at lower pHs Q_A^- becomes a more efficient recombination partner for the S_2 state. Therefore the $S_2Y_DQ_A^- \rightarrow S_1Y_DQ_A$ recombination reaction will dominate in the centers where Q_A^- was present after the flash. This will lower the amplitude of signal II_{slow} (Y_D^+) formed after the flash. The above explanation is supported by the pH-independent amplitude of Y_D^+ formation between pH 8.0 and 6.0 when thylakoid membranes were used (not shown) instead of BBY particles. In thylakoids, the plastoquinone pool is present and the amount of Q_A^- available for recombination with the S_2 state is negligible after a single flash.

Below pH 6.0, the competition of Q_A^- and Y_D for the recombination with the S_2 state is not expected to result in a further drop in the Y_D^+ formation because already at pH 6.0 the recombination of Q_A^- with S_2 is 10 times faster than the electron donation from Y_D to S_2. However, we observed a sudden breakdown in the formation of signal II_{slow} below pH 5.0 (Figure 3B, ×). This effect occurs in the pH range where a low-pH induced inhibition of oxygen evolution takes place (Renger et al., 1976; Schloedder & Meyer, 1987). We have observed this inhibition in our BBY particles (Figure 4), and we suggest that the breakdown of the flash-induced signal II_{slow} amplitude is correlated with the inhibition of the oxygen-evolving complex. The mechanism for the low-pH inhibition is not known; however, preliminary results indicate that the S_1 to S_2 transition is blocked or slowed down below pH 5.0 (not shown). This would decrease the yield for the formation

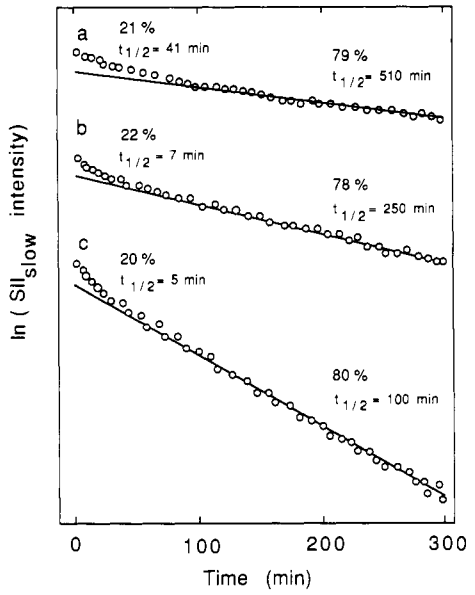

FIGURE 5: Dark decay of signal II_{slow} in BBY particles. The samples were preilluminated with 100 flashes (1-Hz frequency) to oxidize Y_D completely. Then signal II_{slow} was measured in the dark every 3–6 min at room temperature. The intensity of signal II_{slow} is plotted as a function of the decay time at different pHs; a, pH 5.0; b, pH 7.8; c, pH 8.65. EPR conditions were as in Figure 1.

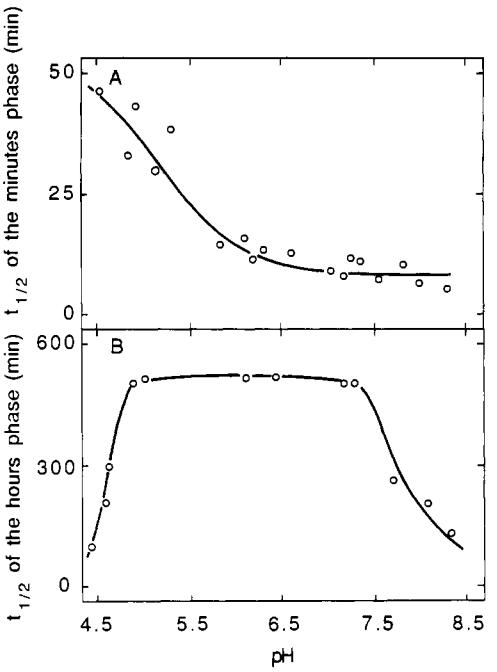

FIGURE 6: pH dependence of the half-times for the decay of signal II_{slow}. The dark decay of signal II_{slow} was measured at several pHs as shown in Figure 5. The half-times calculated for the minutes (A) and the hours (B) phases are plotted as a function of pH.

of the S_2 state that can oxidize Y_D after the flash.

Oxidation of Y_D occurs not only via the S_2 state but also via the S_3 state (Babcock & Sauer, 1973), as indicated by reaction C in Scheme I. The clear separation of Y_D oxidation by the S_2 or S_3 states is complicated by the limited size of the plastoquinone pool in our BBY particles. This effect results in the formation of Q_A^- in part of the centers after one flash and prevents the S_2 to S_3 transition. However, earlier data in the literature show that the oxidation of Y_D by the S_3 state is monophasic at pH 7.5 in thylakoids ($t_{1/2} \approx 1$ s; Babcock & Sauer, 1975) and clearly biphasic at pH 6.3 in BBY particles, with half-times of a few seconds and about 25 s in the presence of the artificial acceptor PPBQ (Styring & Rutherford, 1987). Although a thorough pH study has not been performed on the oxidation of Y_D by the S_3 state, the above literature data indicate a similar pH effect as reported here for the oxidation of Y_D by the S_2 state.

Reduction of Y_D^+ in the Dark. The protonation events that take place either at the water-oxidizing complex or in the vicinity of Y_D are expected to influence the reversed electron transfer as well. Thus, we have measured the pH dependence of the decay kinetics of Y_D^+ (Scheme I, reactions indicated with A and with the unfilled arrow). Samples were first preilluminated by 100 flashes to ensure the complete oxidation of Y_D and the formation of about 25% $S_0Y_D^+$ centers. Then, the kinetics for Y_D^+ reduction were followed by measuring the dark decay of the intensity of signal II_{slow} for several hours at room temperature. As shown in Figure 5, the decay of signal II_{slow} is biphasic, with half-times in the tens of minutes (20–25% relative amplitude) and hours time range (75–80% relative amplitude), respectively. The half-times of both phases are strongly pH dependent (Figure 6). The half-time of the minutes phase increases from about 5 min at pH 8.2 to about 40 min at pH 4.5 (Figure 6A). The hours phase has a constant half-time of 9–10 h between pH 4.7 and 7.2 and decreases abruptly both at the high and low extreme pHs (Figure 6B). Fitting of the measured half-times of the minutes phase by using eq 9, assuming a fast equilibrium of the protons with the bulk solution on the time scale of the experiment, results in pK 5.9 for the monoprotic binding (Figure 6A, solid line).

The decay of signal II_{slow} that occurs in the minutes time scale has a half-time similar to that of the reduction of Y_D^+ by the S_0 state (Styring & Rutherford, 1987; Vass et al., 1990a). In addition, the amplitude of this phase is approximately 25%, which corresponds to the initial population of the $S_0Y_D^+$ centers. Therefore, we assign the minutes phase to the $S_0Y_D^+ \rightarrow S_1Y_D$ process (Scheme I, reaction A). The proton binding with the pK around 5.9 that slows down the above reaction is likely the same event as the one that accelerates the electron transfer in the opposite direction, i.e., in the S_2-$(S_3)Y_D \rightarrow S_1(S_2)Y_D^+$ reaction. This proton was suggested to bind close to the water-oxidizing complex. Thus, the redox state of Y_D (located 20–40 Å away; Evelo et al., 1989b; Svensson et al., 1990) is unlikely to change the pK of that group.

The protonation occurring close to Y_D (presumably at a histidine residue, see above) is also expected to affect the stability of signal II_{slow}. In this case an acceleration of the decay kinetics of Y_D^+ is expected below the pK of the protonizable group. If the pK of this group were the same both in the reduced and oxidized states of Y_D, then we would expect faster reduction kinetics below pH 7.3–7.5. On the other hand, if the pK of the protonizable group is shifted when Y_D is oxidized, as has been suggested for Y_Z ($pK_{ox} \approx 5.0$, $pK_{red} \approx 8.0$; Renger & Voelker, 1982), then the acceleration of the decay of signal II_{slow} is expected to occur below pH 5.0. However, neither of these effects was observed. Above pH 7.5, the oxygen-evolving capacity of the BBY particles is strongly inhibited (Figure 4). Thus, the pure protonation effects could be overlapped by indirect pH effects, preventing the observation of a protonation with pK 7.3–7.5 in the decay of signal II_{slow}. The detection of a destabilization of signal II_{slow} below pH 5.0 (due to a protonation close to Y_D) would be masked by the proton binding with pK 5.8 occurring in the oxygen-evolving complex that increases the stability of signal II_{slow}. However, in this situation the two protonations would have an overlapping effect, one increasing and the other decreasing the rate of the electron transfer from the water-ox-

idizing complex to Y_D^+. This could explain that the pH-induced change in the half-time of the electron transfer is 2–3 times larger for the electron being transferred from Y_D to the water-oxidizing complex (changing from 1 to 20 s, Figure 3A) than in the opposite direction (increasing from 5 to 40 min, Figure 6A).

The hours phase of the decay of signal II_{slow} reflects the reduction of Y_D^+ in the S_1 centers. This can occur by electron transfer from the bulk solution or via equilibrium reactions involving the the S_2Y_D state (see below). The extreme stability of signal II_{slow} between pH 4.7 and 7.2 arises from isolation of the radical from redox-active species in the medium and shows that Y_D is deeply buried in a proteinaceous environment. The dramatic decrease at the low and high pHs in the stability of Y_D^+ (Figure 6B) is likely to be related to the destruction of the water-oxidizing complex via structural changes that make Y_D^+ accessible to redox components in the bulk solution. Y_D^+ is known to be destabilized in the absence of the functional Mn cluster, e.g., in Tris-treated PSII preparations (Lozier & Butler, 1973) or at very low pH (Pulles et al., 1976). Inactivation of oxygen evolution, and release of the functional Mn, is well-known at high pHs (Briantais et al., 1977), and a structural change has been suggested to occur above pH 7.5 (Völker et al., 1985). Below pH 4.5, the oxygen evolution is inhibited in a reaction that is initially reversible (Schloedder & Meyer, 1987) but later results in the release of Mn and irreversible inhibition of oxygen evolution (Pulles et al., 1976). Contrary to this, the decay of Y_D^+ in the pH range between 4.7 and 7.2 is not related to the destruction of the water-oxidizing complex, since the oxygen evolution was much more stable during room temperature incubation than Y_D^+ (results not shown).

Relative Redox Potentials of Y_D and the S States. In the present study we have measured the electron transfer rates in both directions between Y_D/Y_D^+ and the water-oxidizing complex. As depicted in Scheme I, these are equilibrium reactions, and consequently it should be possible to calculate the relative midpoint redox potentials of the involved S states and Y_D if the equilibrium constants could be estimated. The very slow dark decay of Y_D^+ in the S_1 centers can occur either via the direct reduction of Y_D^+ by an unknown electron donor (unfilled arrow in Scheme I) or through S_2Y_D as an intermediary state. Which of these possible processes dominates at physiological pHs is not clear. Via the equilibrium between $S_1Y_D^+$ and S_2Y_D (Scheme I, reaction B), a small population of the centers should always be in the S_2Y_D state. These centers would decay to the S_1Y_D through deactivation of the S_2 state by recombination with acceptor side electrons (Scheme I, $k'_{2,1}$). Assuming that the dominating pathway for the decay of Y_D^+ in the S_1 centers is via the S_2Y_D state, the equilibrium constant between $S_1Y_D^+$ and S_2Y_D, K_B, is given by the ratio of the decay half-times of signal II_{slow} (hours phase) and that of the S_2 state. In our BBY particles the half-decay time of the S_2 state at room temperature is 30–40 s at pH 6.0 (measured by the room-temperature stability of the S_2-state multiline EPR signal, not shown). These data together with the 500-min half-time of Y_D^+ at pH 6.0 (Figure 6A) give a value of 750–1000 for K_B. This equilibrium constant corresponds to a 170–177-mV redox potential difference between the Y_D^+/Y_D and S_2/S_1 couples, the latter couple being the more positive (Figure 7). However, if the direct pathway for the decay of Y_D^+ (Scheme I, unfilled arrow) is faster than the indirect pathway via S_2Y_D, then the above value provides the lowest limit for the redox potential difference. The large value of K_B verifies the assumption made in the theoretical section

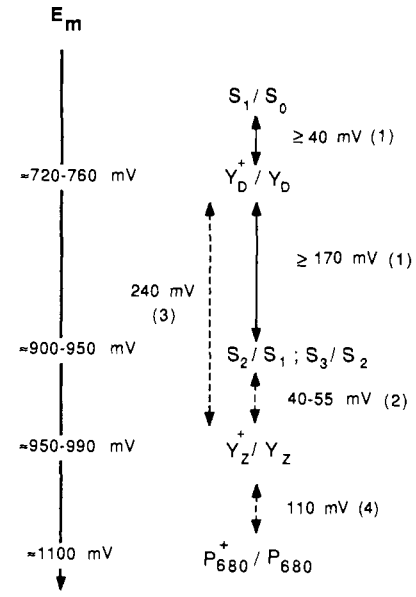

FIGURE 7: Relative midpoint redox potentials for the S_1/S_0, Y_D^+/Y_D, S_2/S_1, S_3/S_2, Y_Z^+/Y_Z, and P_{680}^+/P_{680} couples. The data are from (1) this work, (2) Vos (1990), (3) Boussac and Etienne (1982), and (4) Metz et al. (1989).

concerning the displacement of the equilibrium during the oxidation of Y_D by the S_2 state to the right in Scheme II.

We can also estimate the redox potential difference between the S_1/S_0 and Y_D^+/Y_D couples. The reduction of Y_D^+ by the S_0 state also leads to an equilibrium between the $S_0Y_D^+$ and S_1Y_D states (Scheme I, reaction A). After illumination with continuous light or several flashes, 25% of the centers are expected to be in the $S_0Y_D^+$ state. The relative amplitude of the minutes phase in the decay of signal II_{slow} (which reflects the $S_0Y_D^+ \rightarrow S_1Y_D$ process) is proportional to the concentration of $S_0Y_D^+$ present immediately after the flashes minus the equilibrium concentration of S_1Y_D. In our experiments the amplitude of this phase always varied between 20 and 25% (Figure 6). This indicates that the lowest limit for the K_A equilibrium constant is 5. This corresponds to the Y_D^+/Y_D redox couple being 40 mV or more oxidizing than the S_1/S_0 redox couple (Figure 7).

The equilibrium constant for the electron transfer between Y_D and Y_Z was estimated to be around 10000 (Boussac & Etienne, 1982), which corresponds to a 240-mV midpoint redox potential difference. In addition, the equilibrium constant between Y_Z and the water-oxidizing complex during the S_1 to S_2 transition is about 5, corresponding to a 40-mV redox potential difference between Y_Z^+/Y_Z and S_2/S_1 (Vos, 1990). Our estimation of $E_m(S_2/S_1) - E_m(Y_D^+/Y_D) \geq 170$ mV together with $E_m(Y_Z^+/Y_Z) - E_m(S_2/S_1) \geq 40$ mV results in an approximately 210-mV midpoint redox potential difference between $E_m(Y_Z^+/Y_Z)$ and $E_m(Y_D^+/Y_D)$. This value is in very good agreement with the 240-mV difference obtained from the results of Boussac and Etienne (1982).

A comparison of our results with available literature data makes possible an estimation of the absolute value of $E_m(Y_D^+/Y_D)$ as well. The redox span between $E_m(S_2/S_1)$ and $E_m(Q_A/Q_A^-)$ can be calculated to be about 1030 mV from thermoluminescence measurements (Demeter & Vass, 1984). This value, together with $E_m(Q_A/Q_A^-) \approx -130$ mV (Knaff, 1975) places $E_m(S_2/S_1)$ at around 900 mV [see also Bouges-Bocquet (1980)]. Our estimation of a 170–180-mV redox potential difference between $E_m(S_2/S_1)$ and $E_m(Y_D^+/Y_D)$ results in 720–730 mV for $E_m(Y_D^+/Y_D)$. The approximately 1.1-V E_m of P_{680}^+/P_{680} (Klimov et al., 1979) can also be used

Scheme III

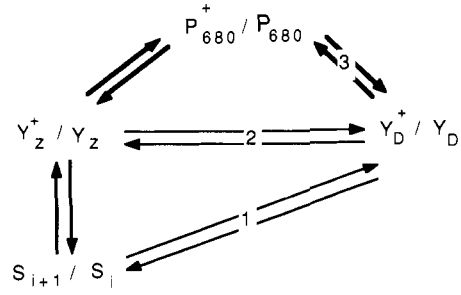

as a reference point for the redox potential estimation of Y_D^+/Y_D. Recently Metz et al. (1989) calculated the E_m-(Y_Z^+/Y_Z) as being 110 mV more negative than the E_m-(P_{680}^+/P_{680}). This result together with $E_m(Y_Z^+/Y_Z) - E_m$-$(S_2/S_1) \approx 40$ mV (Vos, 1990) and with our estimation of $E_m(S_2/S_1) - E_m(Y_D^+/Y_D) \approx 170$–180 mV places $E_m(Y_D^+/Y_D)$ at 770–780 mV. Both of the above estimations for E_m-(Y_D^+/Y_D) are in remarkably good agreement with the 760 mV obtained by Boussac and Etienne (1984). The redox potential values, estimated here or taken from the literature, are summarized in Figure 7. The S_3/S_2 couple is also included and placed very close to the S_2/S_1 couple (Vos, 1990).

We have estimated the redox potential differences at pH 6.0. They can be pH dependent if protonation events directly affect the respective redox transitions. Unfortunately, our experiments allow good estimations only for the lower limits of the midpoint redox potential differences. Therefore, it is not possible to determine their possible pH dependence.

Pathway of Electron Transfer between Y_D and the S States. The data presented here and by previous workers clearly demonstrate the redox interaction between Y_D and the water-oxidizing complex. The pathway for the electron transfer, however, is not clear, and several possibilities exist. Scheme III shows three alternative pathways for the charge exchange between Y_D^+/Y_D and the S states. It can occur in a direct reaction (1), via equilibrium with Y_Z^+/Y_Z (2), or via equilibrium with P_{680}^+/P_{680} involving the equilibrium with Y_Z^+/Y_Z (3). The light-induced formation of signal II_{slow} has been observed in Tris-washed thylakoids (Lozier & Butler, 1973; Babcock & Sauer, 1975; Boussac & Etienne, 1982), in Tris-washed BBY particles (Boussac & Etienne, 1984), and in the low-fluorescent (LF1) mutant of *Scenedesmus* (Rutherford et al., 1988), which lacks the functional Mn cluster. These results show that the presence of the functional Mn cluster is not a prerequisite of the oxidation of Y_D, as also suggested earlier by Boussac and Etienne (1982). Moreover, Y_D was shown to be photooxidizable also in cyanobacterial mutants that lack functional Y_Z and oxygen evolution (Debus et al., 1988b, Metz et al., 1989). These data rule out 1 and/or 2 as the exclusive pathways for the oxidation of Y_D and indicate also that Y_D can donate an electron directly to P_{680}^+. Direct oxidation of Y_D by P_{680}^+ was also suggested by Nugent et al. (1987) and by Miller and Brudvig (1990) under conditions where the electron donation from the water-oxidizing complex to P_{680}^+ is inhibited. The information currently available on the structure of the PSII reaction center indicates that Y_Z and Y_D are most probably arranged symmetrically relative to P_{680} (Babcock et al., 1989; Svensson, 1990). The distance between Y_Z and P_{680} has been estimated to be 10–15 Å (Hoganson & Babcock, 1988). A similar distance can be predicted between Y_D and P_{680} from the symmetry considerations [see also Svensson et al. (1990)]. Contrary to this, the distance between Y_D and the Mn cluster is 20–40 Å (Evelo et al., 1989b). Therefore, it is likely that the interaction of

Scheme IV

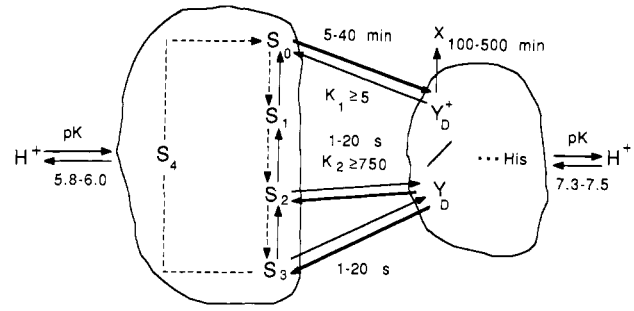

Y_D is stronger with P_{680} than with the water-oxidizing complex.

From these arguments it follows that Y_D is likely to interact with the water-oxidizing complex via a series of charge equilibria (pathway 3 in Scheme III) even in intact systems. The positive charges are stabilized in the water-oxidizing complex in microseconds to milliseconds after the primary charge separation (Rutherford, 1989). However, charge equilibria between the S_2 (S_3) state(s) and Y_Z and P_{680} maintain a low concentration of P_{680}^+ in the dark. This is corroborated by the occurrence of charge recombination between $S_2Q_A^-$ and $S_3Q_A^-$ (Sane & Rutherford, 1986). The equilibrium concentration of P_{680}^+ can oxidize Y_D in seconds at the expense of positive charges stored in the water-oxidizing complex. In the S_0 state, P_{680}^+, maintained by the equilibrium with Y_D^+, can oxidize the S_0 state to S_1 at the expense of positive charges stored on Y_D^+.

Concluding Remarks. The main results presented in this paper are summarized in Scheme IV. The electron transfer reaction from Y_D to the water-oxidizing complex in the S_2 state occurs with a pH-dependent rate constant. The half-time for the reaction varies between 1 s at pH 8.0 to about 20 s at pH 5.0 [literature data indicate that the electron transfer from Y_D to the S_3 state shows a similar pH dependence (Babcock & Sauer, 1973; Styring & Rutherford, 1987)]. The electron transfer from the S_0 state to Y_D^+ also depends on the pH. The half-time for that reaction is 5 min at pH 8.0 and approximately 40 min at pH 5.0. The electron transfer reactions are influenced by two separate protonation events that occur either close to Y_D or in the vicinity of the water-oxidizing complex.

The protonation in the vicinity of Y_D ($pK \approx 7.3$–7.5) retards the electron transfer from Y_D to the S_2 (or S_3) state(s) nearly by a factor of 20. This effect is very similar to the effect of pH on the electron transfer rate from Y_Z to P_{680}^+. In Tris-washed BBY particles, this reaction occurs with a half-time of 30 μs at pH 4.5 and 1–3 μs at pH 7.5 (Conjeaud & Mathis, 1986; Schlodder & Meyer, 1987). The pK for the protonation in the vicinity of Y_Z was estimated to be around 6.5 (Conjeaud & Mathis, 1986), which value is quite similar to the pK = 7.3–7.5 observed for the protonation around Y_D (Scheme IV). We have recently used computer modeling to predict the three-dimensional structure around Y_D and Y_Z (Svensson et al., 1990). One of the most striking features of the predicted structure is that both Y_D and Y_Z are likely to form hydrogen bonds to a nearby histidine residue (His-190 of the D2 and the D1 protein, respectively). The observation here of an amino acid residue with $pK \approx 7.3$–7.5 in the vicinity of Y_D is the first experimental support for the suggestion that Y_D forms a hydrogen bond with His-190. In addition, the presence of the hydrogen bond between Y_Z and His-190 of the D1 protein is supported by the existence of a group close to Y_Z that is protonated with $pK \approx 6.5$ (Conjeaud & Mathis, 1986). The presence of a hydrogen bond between Y_Z and a neighboring amino acid was also suggested by Eckert and Renger

(1988) from the temperature dependence of the rate of the $Y_Z \rightarrow P_{680}^+$ electron transport.

The protonation in or close to the water-oxidizing complex, which occurs with a pK of 5.8–6.0, accelerates the electron transfer from Y_D to S_2 (and S_3) and retards the electron transfer from S_0 to Y_D^+. In this respect, this protonation behaves similarly to a protonation at the level of the water-oxidizing complex that retards the electron transfer from Y_Z to P_{680}^+ (Meyer et al., 1989). The measured pKs for the two reactions differ somewhat [pK = 5.8–6.0 in our case, pK = 5.3 in the case of Meyer et al. (1989)], but we propose that the same protonation is responsible for both effects. The nature of that acidic group is not known. The pK may reflect protonation of an amino acid side chain in the vicinity of the Mn cluster involved in the oxidation of water or, as was proposed by Meyer et al. (1989), the protonation of H_2O on the site.

Finally, Scheme IV shows the very slow reduction of Y_D^+ via a partly undefined pathway. Between pH 4.7 and 7.2 this reaction occurs with a half-time of about 500 min [compare also Figure 4 in Babcock and Sauer (1973)]. At pHs that inactivate the water-oxidizing complex, the stability of Y_D^+ is much decreased, similarly to what has been found earlier in Tris-washed chloroplasts (Lozier & Butler, 1973). Electrons from the acceptor side of PSII could be involved in the slow reduction of Y_D^+ at physiological pHs. One possible pathway for that reaction is the equilibrium of the $S_1Y_D^+$ and S_2Y_D centers, followed by their conversion to S_1Y_D via recombination of the S_2 state with acceptor-side electrons. Another pathway could involve cytochrome *b*-559 as intermediary state. We have recently demonstrated that Y_D^+ can be reduced by the high potential form of cyt *b*-559 in a very slow process at 195 K (Vass et al., 1990b). The reaction is faster at 250 K (not shown) and may take place at room temperature as well. Net oxidation of cyt *b*-559 is not expected at room temperature because it would be rereduced by electrons from the plastoquinone pool (Tsujimoto & Arnon, 1985).

Added in Proof

After the acceptance of this manuscript, we became aware of a study of the oxidation kinetics of Y_D in Mn-depleted PSII membranes (Buser et al., 1990). Their results agree with our conclusion that Y_D directly interacts with P_{680}^+, whose population is maintained in the dark via redox equilibria with Y_Z^+ and with the Mn cluster. However, in contrast to our direct kinetic measurements, showing a proton binding (pK = 7.3–7.5) close to Y_D that is expected to result in a pH-dependent electron transfer rate between Y_D and P_{680}^+, the global fit of the data of Buser et al. (1990) do not indicate such a pH dependence. This apparent discrepancy might be caused by an alteration of the protein structure around Y_D in the Mn-depleted PSII membranes modifying the interaction with the protonated amino acid residue observed in the intact membranes used in our study.

Acknowledgments

We appreciate stimulating discussion with Dr. G. Babcock. The valuable technical assistance of Torbjörn Astlind and Anna Maria Tomka is gratefully acknowledged.

References

Andersson, B., Sayre, R. T., & Bogorad, L. (1987) *Chem. Scr. 27B*, 195–200.

Andrêasson, L.-E., & Vänngård, T. (1988) *Annu. Rev. Plant Physiol. Plant Mol. Biol. 39*, 379–411.

Babcock, G. T. (1987) in *Photosynthesis* (Amesz, J., Ed.), Vol. 15, New Comprehensive Biochemistry, pp 125–158, Elsevier, Amsterdam, The Netherlands.

Babcock, G. T., & Sauer, K. (1973) *Biochim. Biophys. Acta 325*, 483–503.

Babcock, G. T., & Sauer, K. (1975) *Biochim. Biophys. Acta 396*, 48–62.

Babcock, G. T., Barry, B. A., Debus, R. J., Hoganson, C. W., Atamian, M., McIntosh, L., Sithole, I., & Yocum, C. F. (1989) *Biochemistry 28*, 9557–9565.

Berthold, D. A., Babcock, G. T., & Yocum, C. F. (1981) *FEBS Lett. 61*, 231–234.

Blankenship, R. E., Babcock, G. T., Warden, J. T., & Sauer, K. (1975) *FEBS Lett. 51*, 287–293.

Bouges-Bocquet, B. (1980) *Biochim. Biophys. Acta 594*, 85–103.

Boussac, A., & Etienne, A. L. (1982) *Biochem. Biophys. Res. Commun. 109*, 1200-1205.

Boussac, A., & Etienne, A. L. (1984) *Biochim. Biophys. Acta 766*, 576–581.

Brettel, K., Schlodder, E., & Witt, H. T. (1984) *Biochim. Biophys. Acta 766*, 403–415.

Briantais, J.-M., Vernotte, C., Lavergne, J., & Arntzen, C. J. (1977) *Biochim. Biophys. Acta 461*, 61–74.

Brudvig, G. W., Beck, W. F., & dePaula, J. C. (1989) *Annu. Rev. Biophys. Biophys. Chem. 18*, 25–46.

Buser, C. A., Thompson, L. K., Diner, B. A., & Brudvig, G. W. (1990) *Biochemistry 29*, 8977–8985.

Casey, J. L., & Sauer, K. (1984) *Biochim. Biophys. Acta 767*, 21–28.

Conjeaud, H., & Mathis, P. (1986) *Biophys. J. 49*, 1215–1221.

Debus, R. J., Barry, B. A., Babcock, G. T., & McIntosh, L. (1988a) *Proc. Natl. Acad. Sci. U.S.A. 85*, 427–430.

Debus, R. J., Barry, B. A., Sithole, I., Babcock, G. T., & McIntosh, L. (1988b) *Biochemistry 27*, 9071–9074.

Demeter, S., & Vass, I. (1984) *Biochim. Biophys. Acta 764*, 24–32.

Dismukes, G. C., & Siderer, Y. (1980) *FEBS Lett. 121*, 78–80.

Eckert, H.-J., & Renger, G. (1988) *FEBS Lett. 236*, 425–431.

Evelo, R. G., Dikanov, S. A., & Hoff, A. J. (1989a) *Chem. Phys. Lett. 159*, 25–30.

Evelo, R. G., Styring, S., Rutherford, A. W., & Hoff, A. J. (1989b) *Biochim. Biophys. Acta 973*, 428–442.

Förster, V., & Junge, W. (1984) in *Photosynthesis Research* (Sybesma, C., Ed.) Vol. 2, pp 305–308, Martinus Nijhoff/Dr. W. Junk Publishers, Dordrecht, The Netherlands.

Fowler, C. F. (1977) *Biochim. Biophys. Acta 462*, 414–421.

Franzên, L.-G., Hansson, Ö., & Andrêasson, L.-E. (1985) *Biochim. Biophys. Acta 808*, 171–179.

Hansson, Ö., & Wydrzysnki, T. (1990) *Photosynth. Res. 23*, 131–162.

Hansson, Ö., Aasa, R., & Vänngård, T. (1987) *Biophys. J. 51*, 825–832.

Hoganson, C. W., & Babcock, G. T. (1988) *Biochemistry 27*, 5848–5855.

Klimov, V. V., Allakhverdiev, S. I., Demeter, S., & Krasnovsky, A. A. (1979) *Dokl. Akad. Nauk. SSSR 249*, 227–230.

Knaff, D. B. (1975) *FEBS Lett. 60*, 331–335.

Kok, B., Forbush, B., & McGloin, M. (1970) *Photochem. Photobiol. 11*, 457–475.

Lozier, R. H., & Butler, W. L. (1973) *Photochem. Photobiol. 17*, 133–137.

Mei, R., Green, J. P., Sayre, R. T., & Frasch, W. D. (1989) *Biochemistry 28*, 5560–5567.

Metz, J. G., Nixon, P. J., Rögner, M., Brudvig, G. W., & Diner, B. A. (1989) *Biochemistry 28*, 6960–6969.
Meyer, B., Schlodder, E., Dekker, J. P., & Witt, H. T. (1989) *Biochim. Biophys. Acta 974*, 36–43.
Miller, A.-F., & Brudvig, G. (1990) *Biochemistry 29*, 1385–1392.
Nanba, O., & Satoh, K. (1987) *Proc. Natl. Acad. Sci. U.S.A. 84*, 109–112.
Nugent, J. H. A., Demetriou, C., & Lockett, C. J. (1987) *Biochim. Biophys. Acta 894*, 534–542.
Pulles, M. P. J., van Gorkom, H. J., & Verschoor, A. M. (1976) *Biochim. Biophys. Acta 440*, 98–106.
Renger, G., & Völker, M. (1982) *FEBS Lett. 187*, 224–226.
Renger, G., Gläser, M, & Buchwald, H. E. (1976) *Biochim. Biophys. Acta 461*, 392–402.
Robinson, H. H., & Crofts, A. R. (1984) in *Advances in Photosynthesis Research*, Proceedings of the 6th International Congress on Photosynthesis, Brussels, Belgium, August 1983 (Sybesma, C., Ed.) Vol. 1, pp 477–480, Martinus Nijhoff, Dordrecht, The Netherlands.
Rodriguez, I. D., Chandrasekar, T. K., & Babcock, G. T. (1987) in *Progress in Photosynthesis Research* (Biggins, J., Ed.) Vol. 1, pp 471–474, Martinus Nijhoff Publishers, Dordrecht, The Netherlands.
Rutherford, A. W. (1989) *Trends Biochem. Sci. 14*, 227–232.
Rutherford, A. W., Seibert, M., & Metz, J. G. (1988) *Biochim. Biophys. Acta 932*, 171–176.
Sane, P. V., & Rutherford, A. W. (1986) in *Light Emission by Plants and Bacteria* (Govindjee, Amesz, J., & Fork, D. C., Eds.) pp 329–360, Academic Press, Orlando, FL.
Schlodder, E., & Meyer, B. (1987) *Biochim. Biophys. Acta 890*, 23–31.
Seibert, M., Tamura, N., & Inoue, Y. (1989) *Biochim. Biophys. Acta 974*, 185–191.
Styring, S., & Rutherford, A. W. (1987) *Biochemistry 26*, 2401–2405.
Styring, S., & Rutherford, A. W. (1988) *Biochemistry 27*, 4915–4923.
Svensson, B., Vass, I., Cedergren, E., & Styring, S. (1990) *EMBO J. 9*, 2051–2059.
Tso, J., Hunziker, D., & Dismukes, G. C. (1987) in *Progress in Photosynthesis Research* (Biggins, J., Ed.) Vol. 1, pp 487–490, Martinus Nijhoff Publishers, Dordrecht, The Netherlands.
Tsujimoto, H. Y., & Arnon, D. I. (1985) *FEBS Lett. 179*, 51–54.
Vass, I, & Inoue, Y. (1986) *Photosynth. Res. 10*, 432–436.
Vass, I., Deák, Zs., & Hideg, É. (1990a) *Biochim. Biophys. Acta 1017*, 63–69.
Vass, I., Deák, Zs., Jegerschöld, C., & Styring, S. (1990b) *Biochim. Biophys. Acta 1018*, 41–46.
Velthuys, B. R., & Visser, J. W. M. (1975) *FEBS Lett. 55*, 109–112.
Vermaas, W. F. J., Renger, G., & Dohnt, G. (1984) *Biochim. Biophys. Acta 764*, 194–202.
Vermaas, W. F. J., Rutherford, A. W., & Hansson, Ö. (1988) *Proc. Natl. Acad. Sci. U.S.A. 85*, 8477–8481.
Virgin, I., Styring, S., & Andersson, B. (1988) *FEBS Lett. 233*, 408–412.
Vos, M. (1990) Ph.D. Thesis, University of Leiden, Leiden, The Netherlands.
Völker, M., Ono, T., Inoue, Y., & Renger, G. (1985) *Biochim. Biophys. Acta 806*, 25–34.
Zimmermann, J. L., & Rutherford, A. W. (1984) *Biochim. Biophys. Acta 767*, 160–167.